

Fig. 1. Schematic diagram of urban rain flood inundation principle. (Compared with natural watersheds, the underlying surface conditions of cities are more complicated. Urban floods also include three parts: pipe network overflow, river overflow, and surface overflow.)

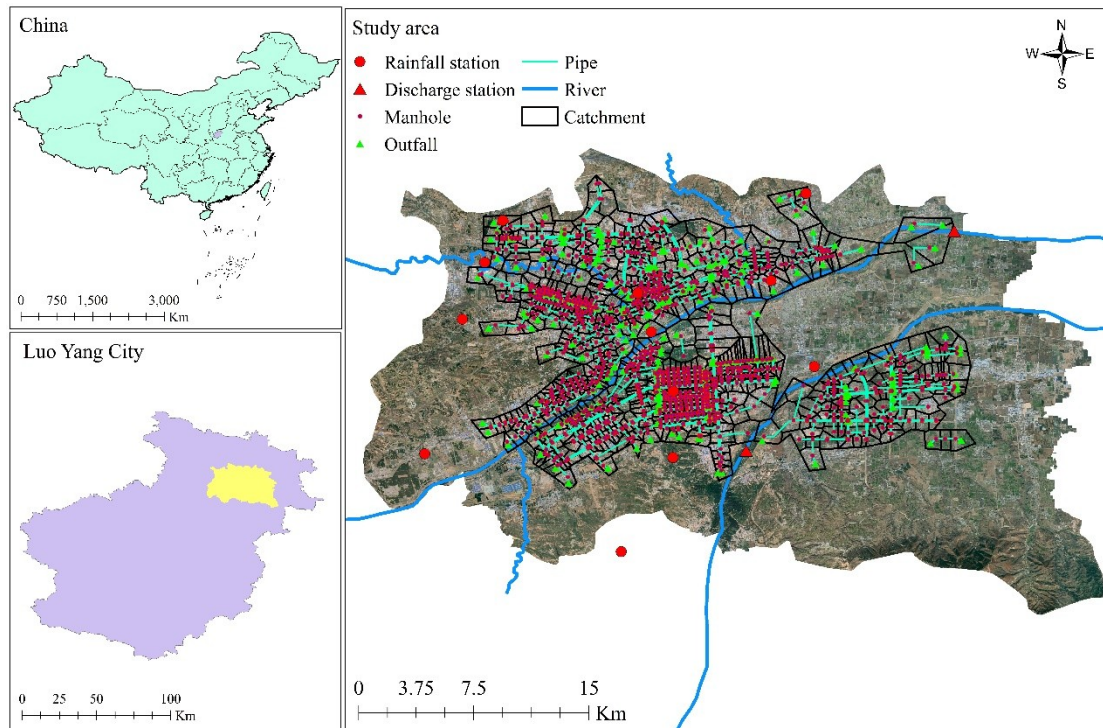


Fig. 2. Research region and sewer system distribution. We selected Luoyang city center, in the northern Henan Province of China, as our study area ($34^{\circ}29'06''$ - $34^{\circ}45'47''$ N, $112^{\circ}15'44''$ - $112^{\circ}41'57''$ E, at 150 m asl) (Fig. 1). Luoyang city center, which constitutes the northern part of Luoyang city, is a typical

small basin city with an area of 803 km², and is situated within the Yi-Luo River Basin. The two rivers of Yi he and Luo he passed through the downtown area of Luoyang.

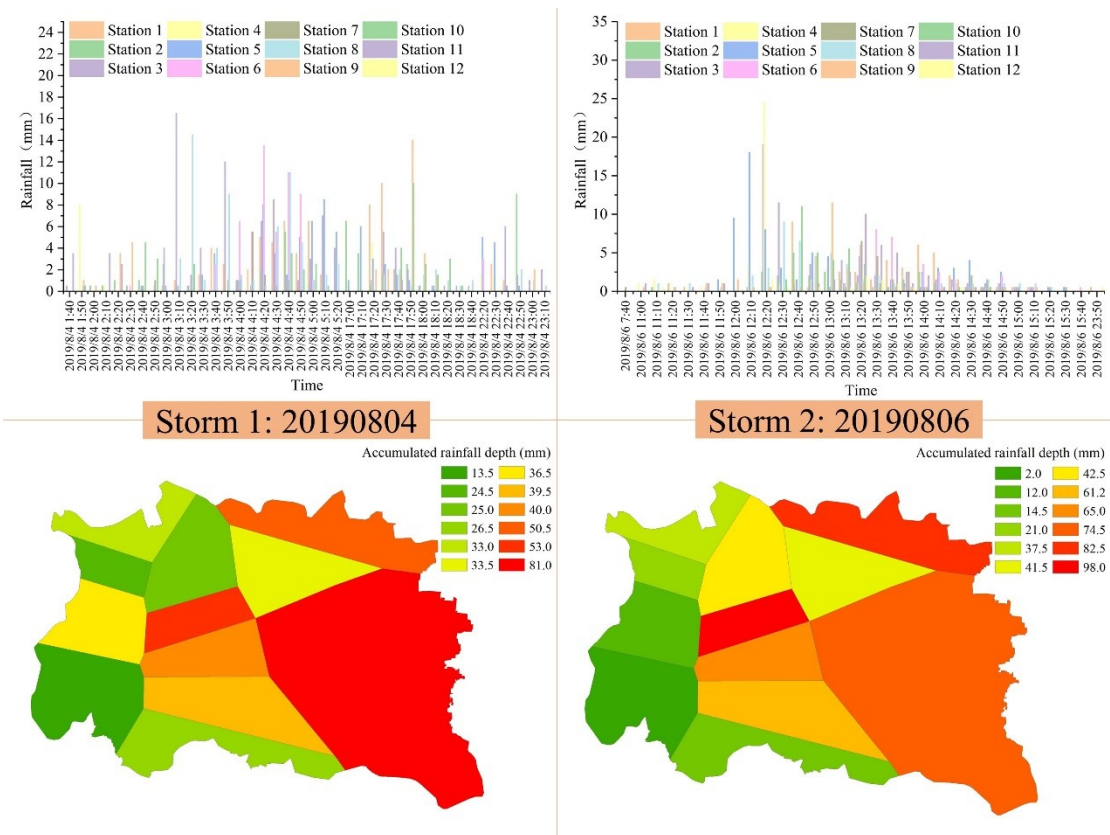


Fig. 3. Hydrographs of the two historical rainstorms (August 4, 2019 and August 6, 2019). Storm 1 started at 1:40 and ended at 23:10 on August 4, 2019. It is a unimodal rainstorm, the first rainfall peak occurred at 3:10 with an intensity of 16.5 mm/h and the second rainfall peak occurred at 17:30 with an intensity of 5.5 mm/h. Storm 2 started at 7:40 and ended at 23:50 lasted about 22h on August 6, 2019 with the maximum intensity of 24.0 mm/h occurred at 12:20. Fig. 3 shows the hydrographs of the storms.

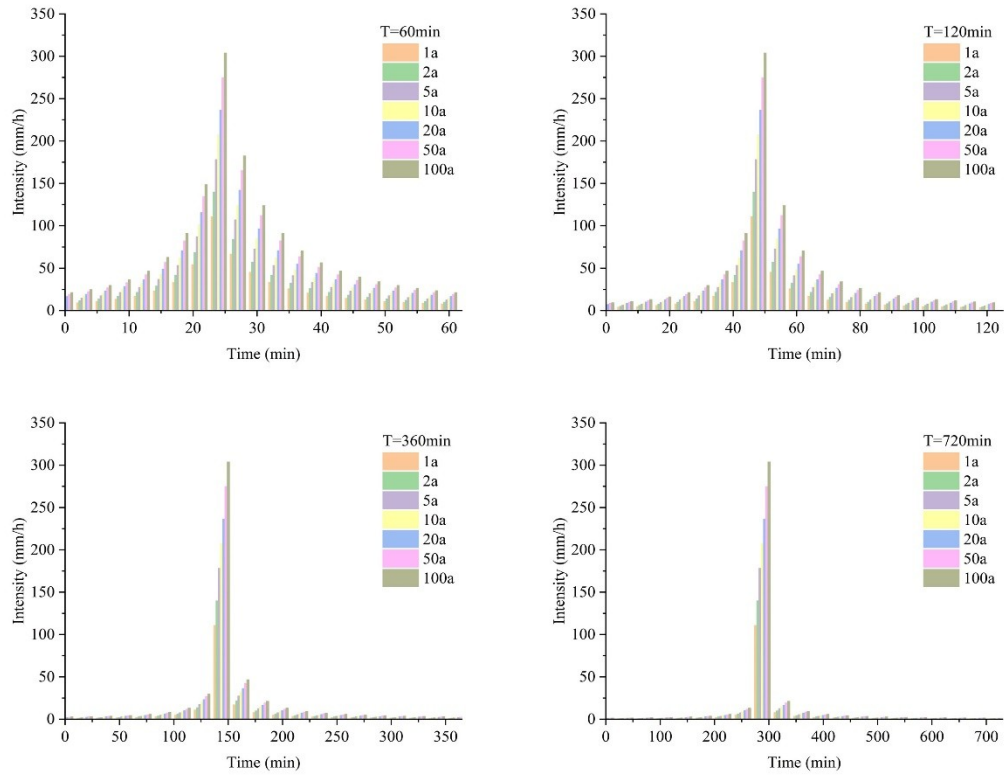


Fig. 4. Synthetic hyetograph of four rainstorm patterns. The main difference among the four rainstorm patterns is the position of the rainfall duration, the rainfall duration were set to 60min, 120min, 360min, and 720min (Fig.4). We named these four rainstorms (Fig.4) as Pattern 1, Pattern 2, Pattern 3, and Pattern 4.

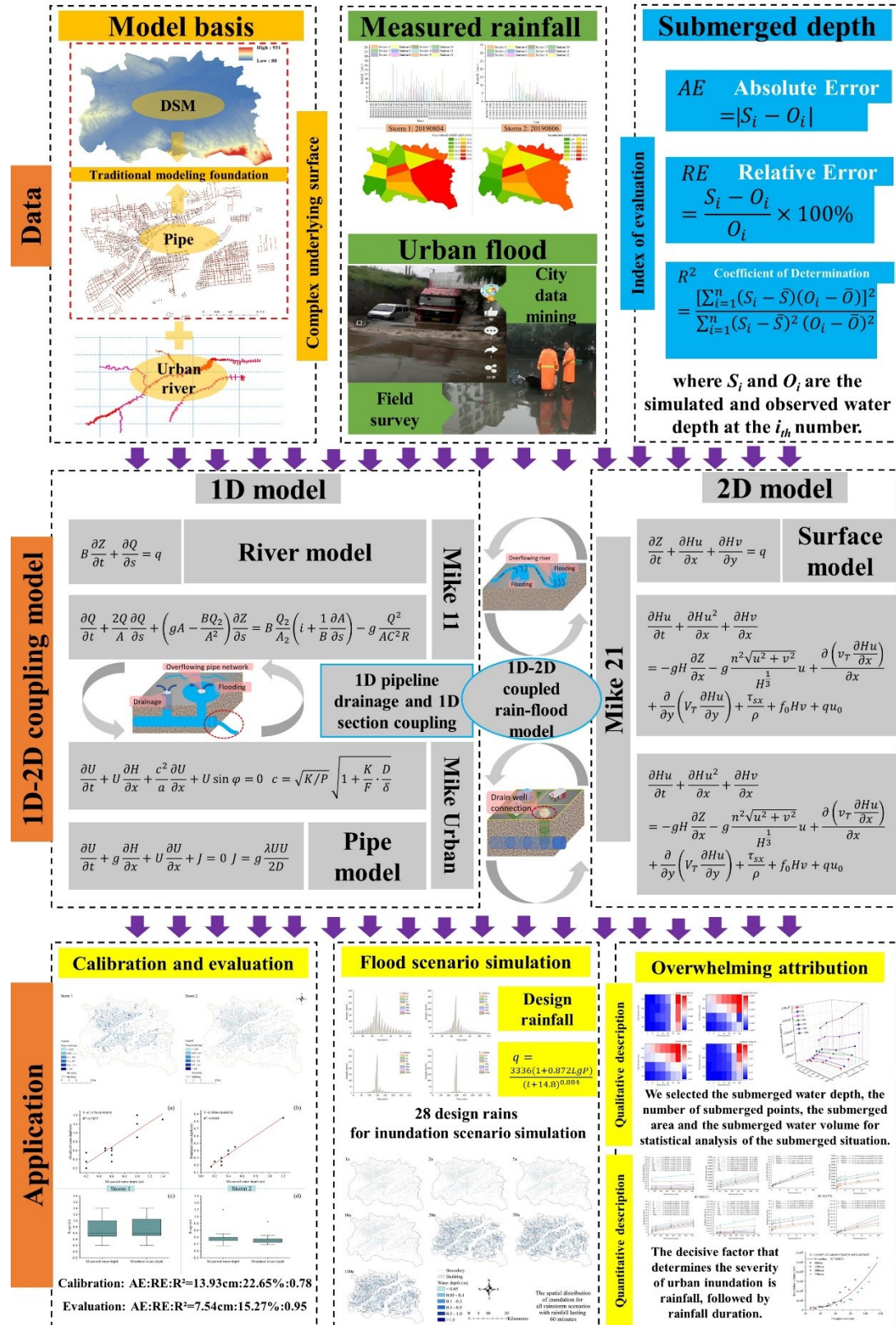


Fig. 5 1D-2D rainfall flood model coupling scheme (The process frame diagram of this study)

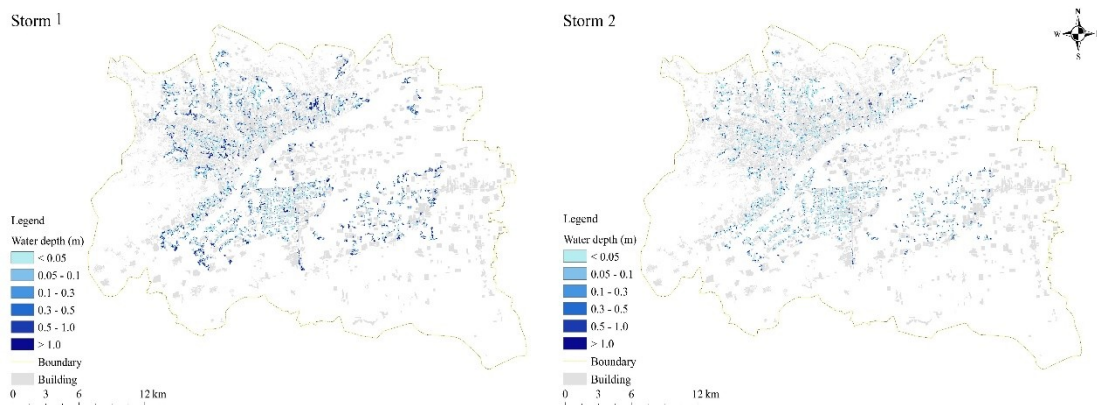


Fig. 6. Spatial distributions of inundations from Storm 1 and Storm 2.

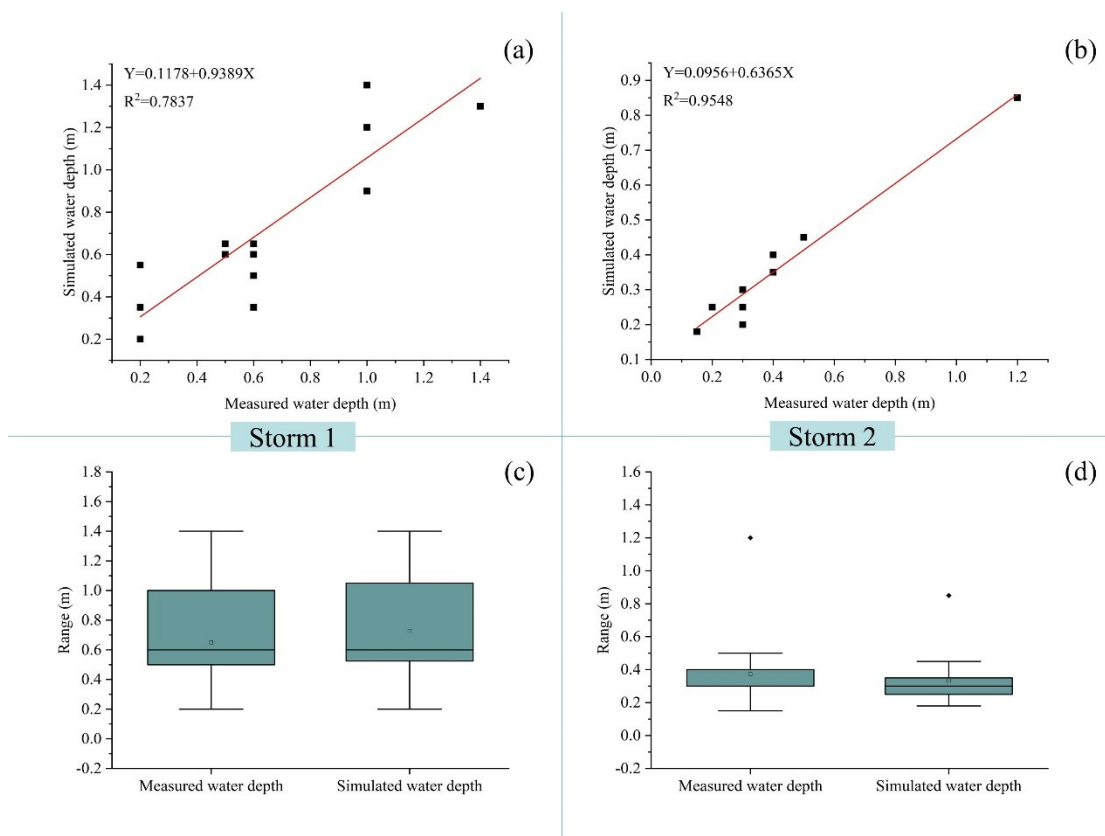


Fig. 7. Comparison of simulated water depth and measured water depth of Storm 1 and Storm 2.

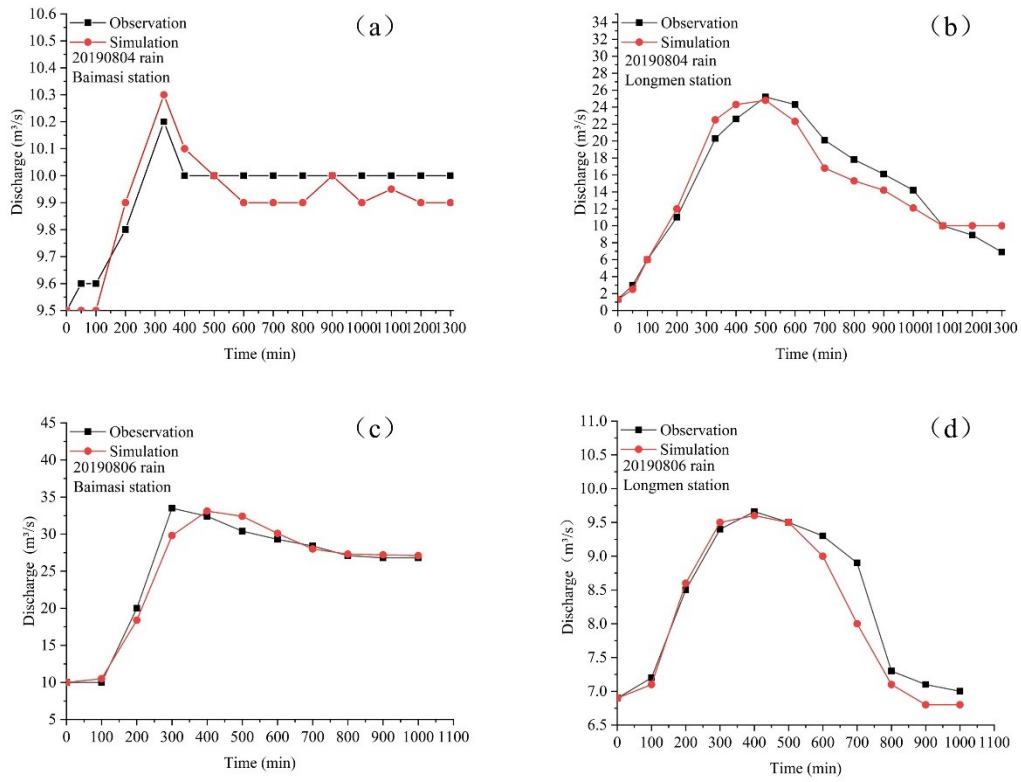


Fig. 8. Comparison of simulated discharge and observed discharge of Storm 1 and Storm 2: (a) Discharge calibration of 20190804 rain in Baimasi station; (b) Discharge calibration of 20190804 rain in Longmen station; (c) Discharge evaluation of 20190806 rain in Baimasi station; (d) Discharge evaluation of 20190806 rain in Longmen station

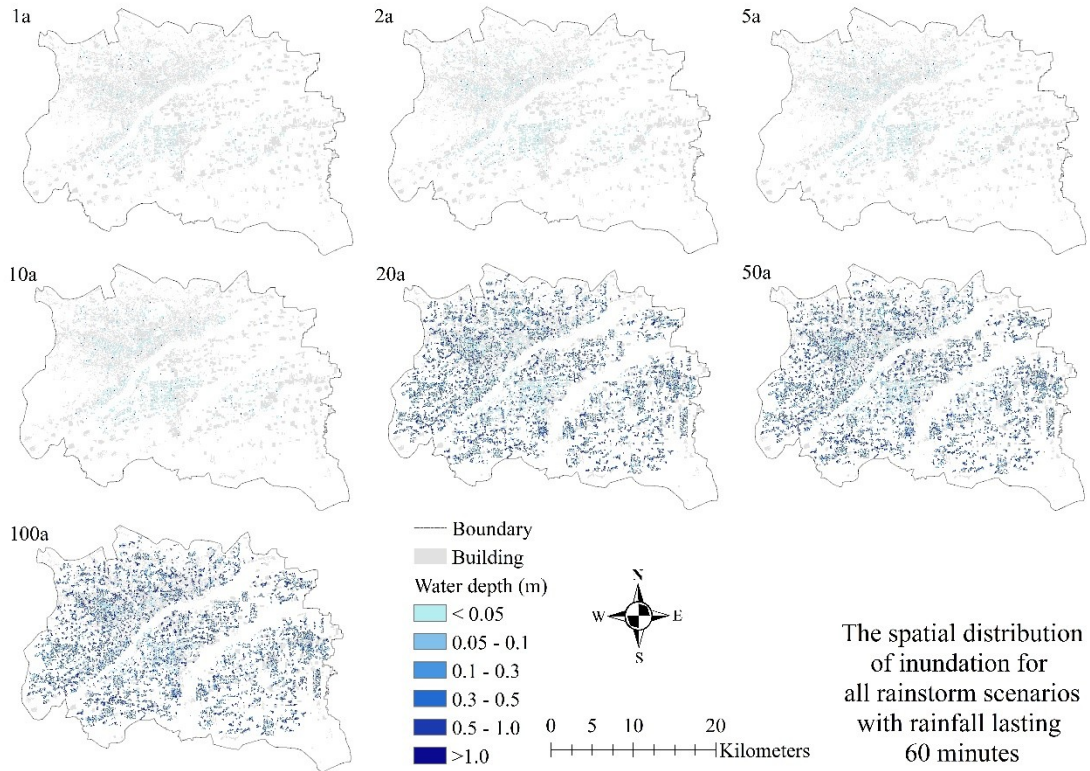


Fig. 9. Spatial distributions of inundation for 60min rainstorm scenarios.

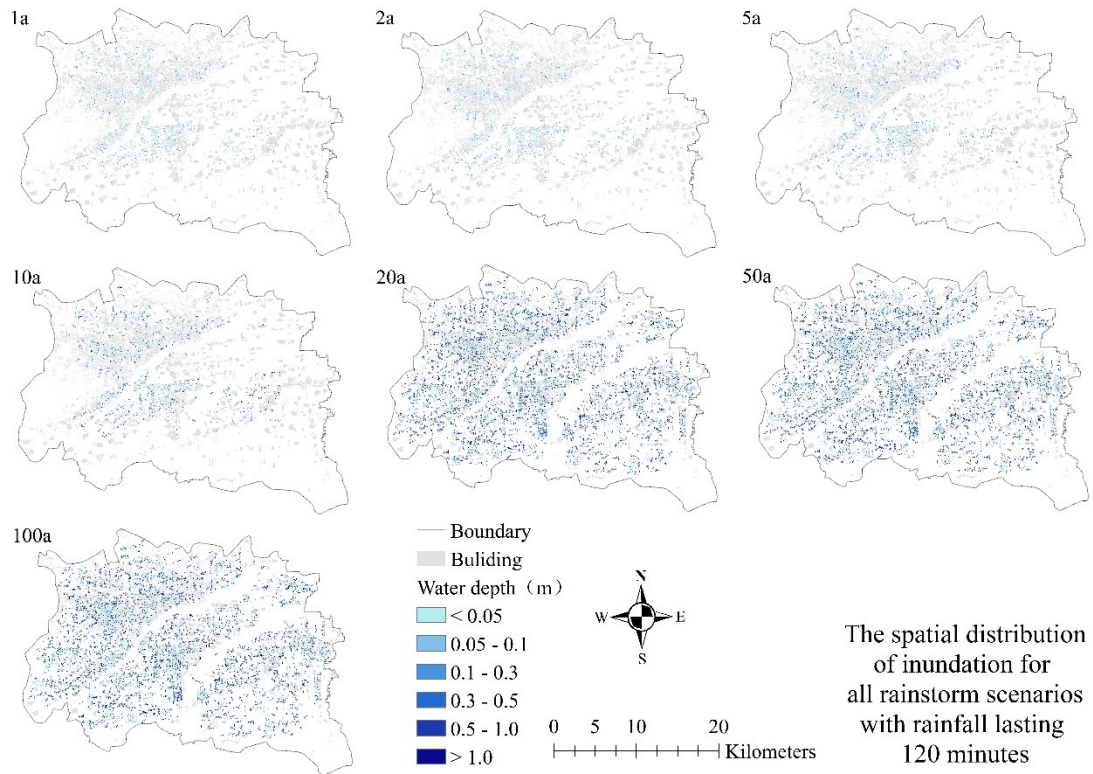


Fig. 10. Spatial distributions of inundation for 120min rainstorm scenarios.

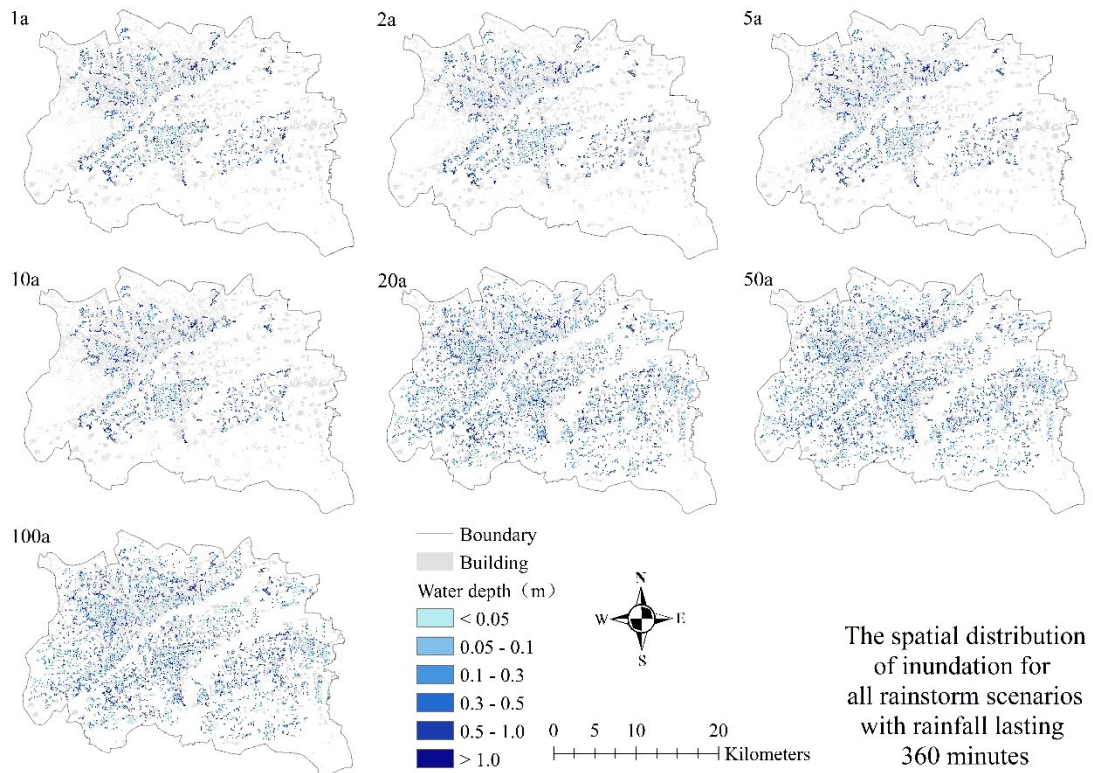


Fig. 11. Spatial distributions of inundation for 360min rainstorm scenarios.

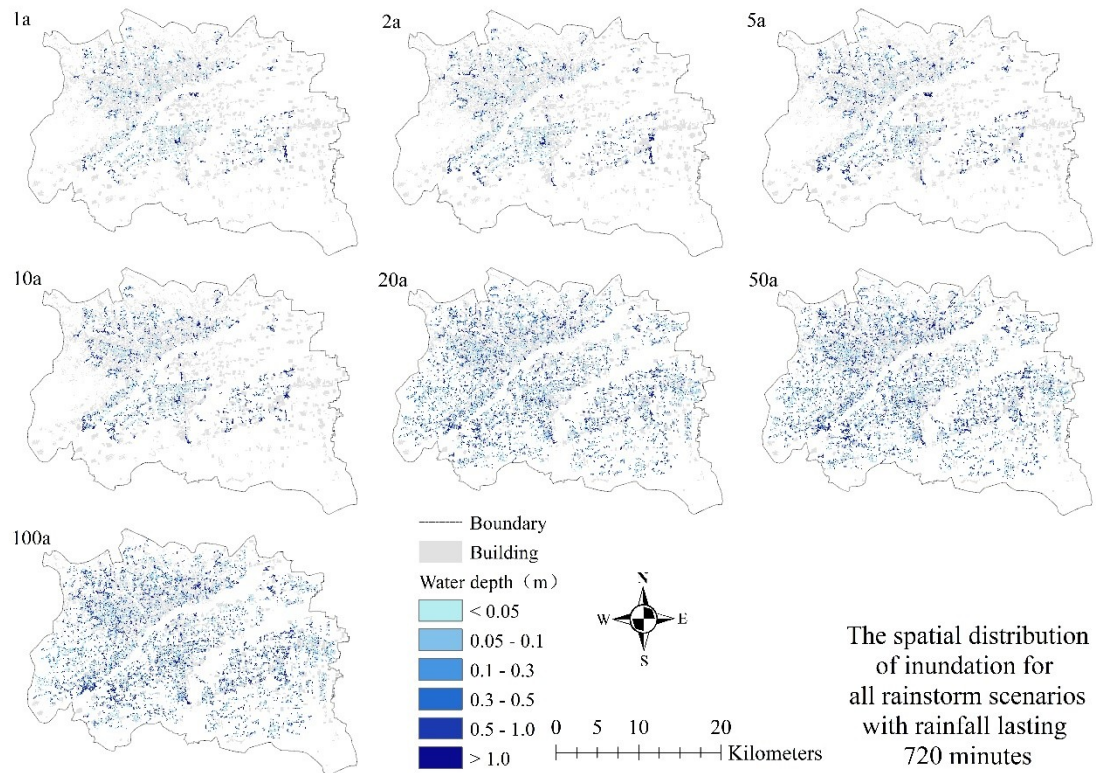


Fig. 12. Spatial distributions of inundation for 720min rainstorm scenarios.

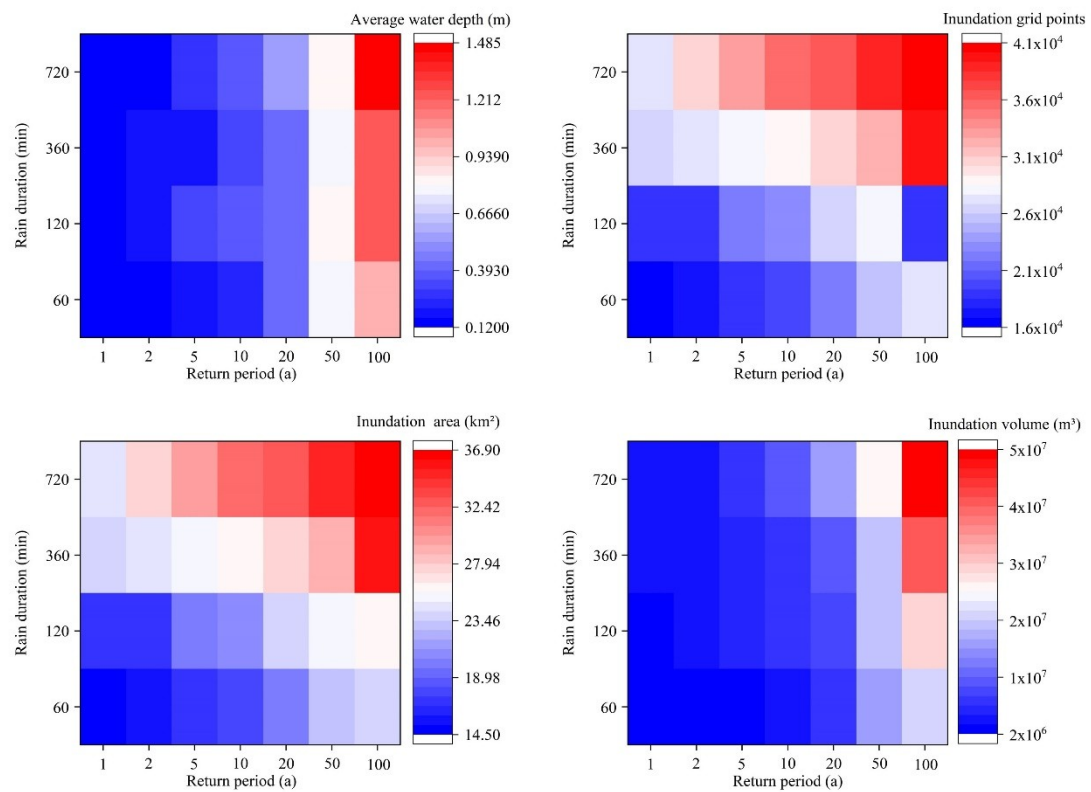


Fig. 13. (a)The relationship between the average submerged water depth and the return period and duration of rainfall. (b)The relationship between the number of submerged grid points and the rainfall return period and rainfall duration. (c)The relationship between submerged area and rainfall return

period and rainfall duration. (d)The relationship between submerged water volume and rainfall return period and rainfall duration.

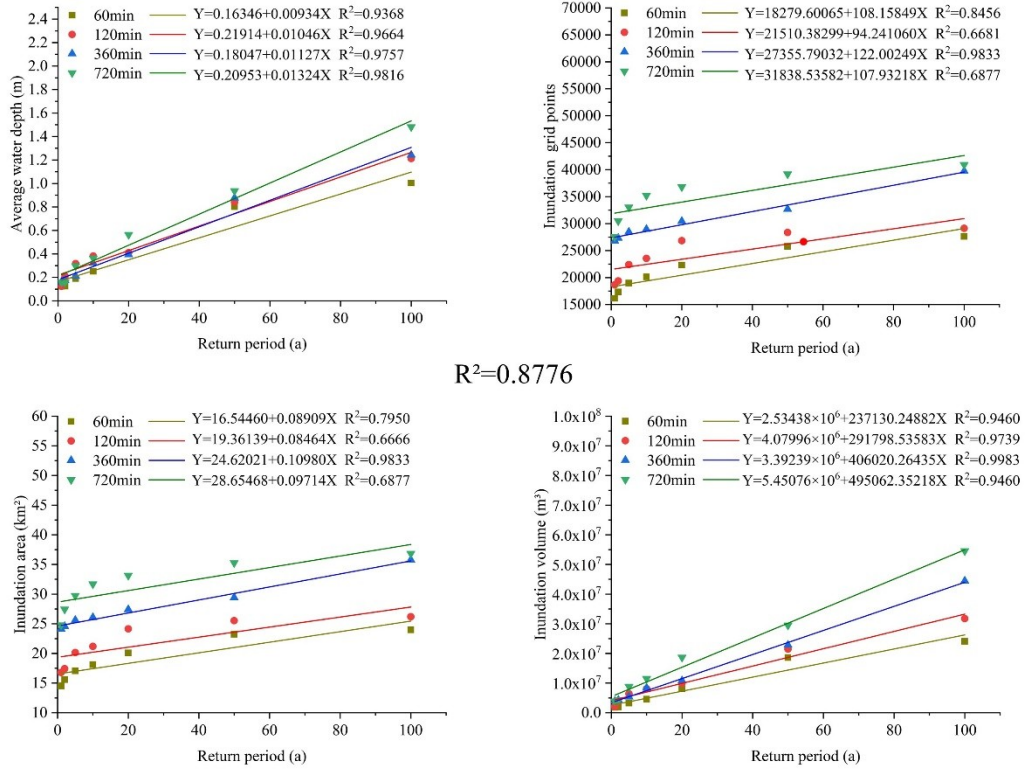


Fig. 14. Trend chart of relationship between submerged water depth, submerged grid points, submerged area, submerged water volume and return period. (The return period and the four submergence indicators are linearly correlated, with an average R^2 of 0.8776.)

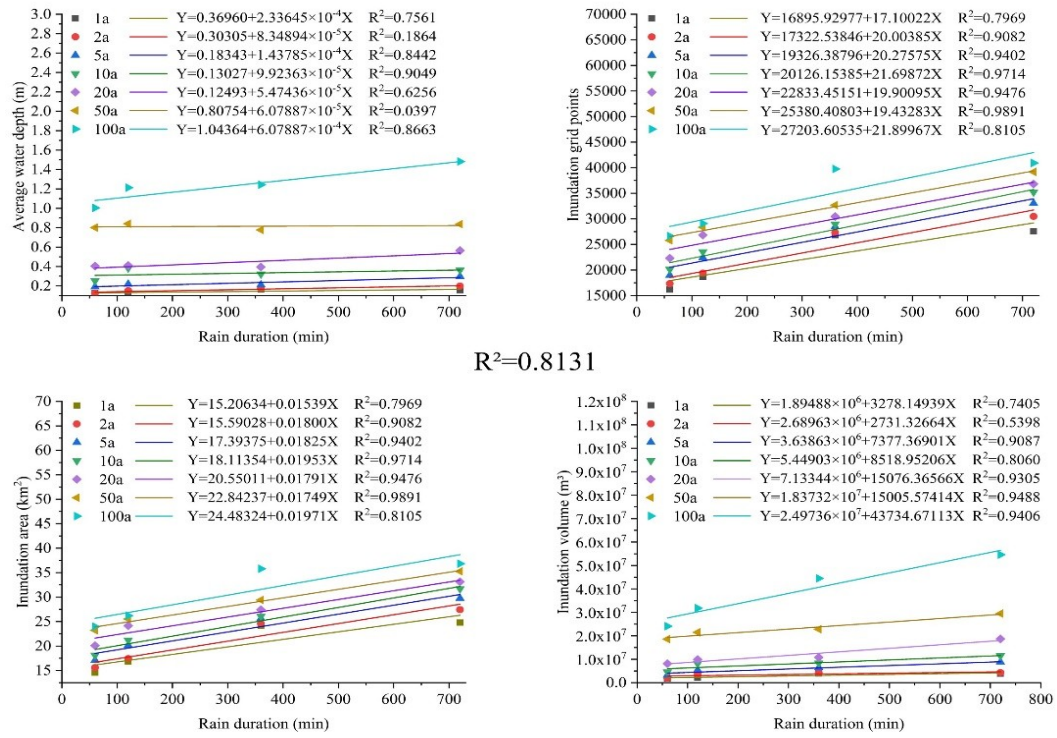


Fig. 15. Trend chart of relationship between submerged water depth, submerged grid points, submerged area, submerged water volume and rain duration. (The rain duration and the four submergence indicators are linearly correlated, with an average R^2 of 0.8131.)

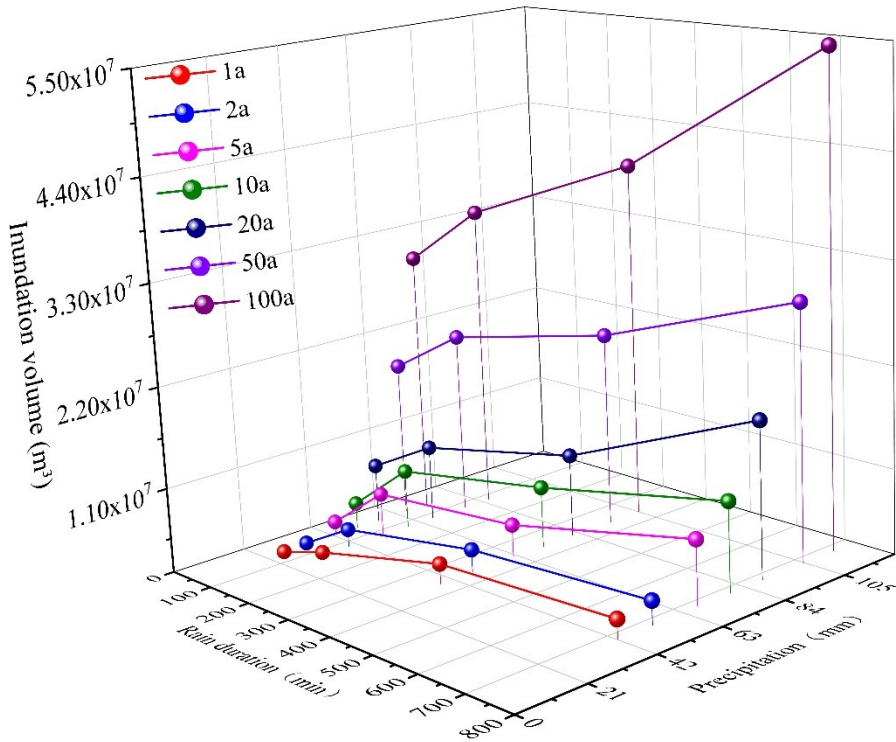


Fig. 16. The relationship between submerged water volume and rainfall duration and rainfall.

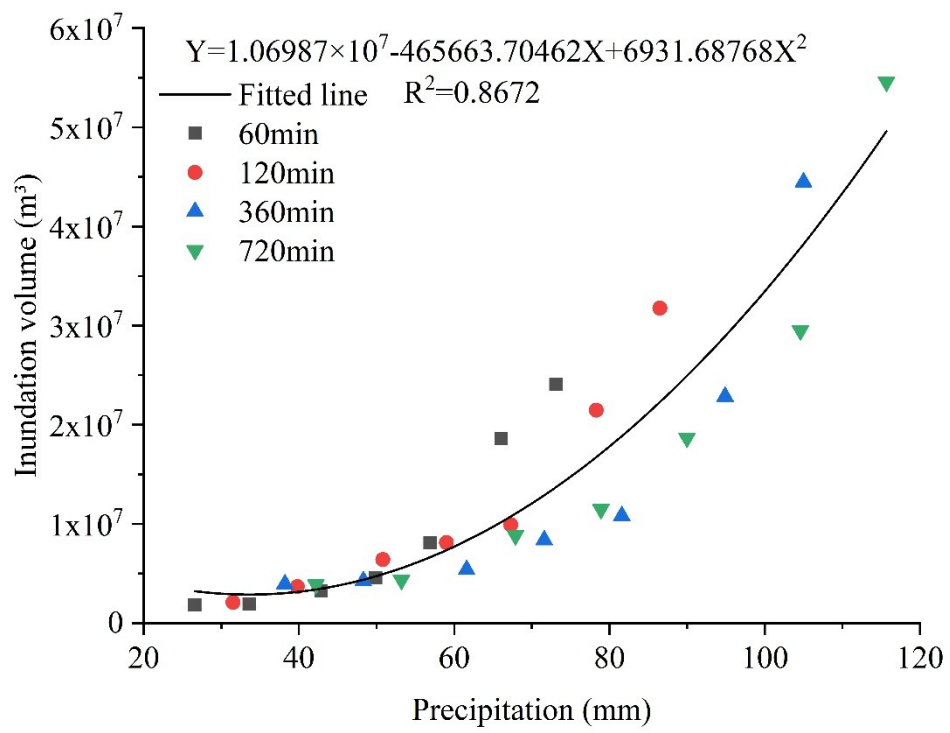


Fig. 17. The relationship between submerged water volume and rainfall.